Self-consistency iterations in electronic-structure calculations

P. H. Dederichs and R. Zeller
Institut für Festkörperforschung der Kernforschungsanlage Jülich, D-5170 Jülich, West Germany
(Received 15 February 1983; revised manuscript received 25 July 1983)

The convergence of self-consistency iterations in electronic-structure calculations based on density-functional theory is examined by the linearization of the self-consistency equations around the exact solution. In particular, we study the convergence of the usual procedure employing a mixture of the input and output of the last iteration. We show that this procedure converges for a suitably chosen mixture. However, the convergence is necessarily slow in certain cases. These problems are connected either with large charge oscillations or with the onset of magnetism. We discuss physical situations where such problems occur. Moreover, we propose some improved iteration schemes which are illustrated in calculations for 3*d* impurities in Cu.

I. INTRODUCTION

In electronic-structure calculations one is faced with a self-consistency problem for the charge density $\rho(\vec{r})$. In density-functional theory[1] the charge density

$$\rho(\vec{r})=\sum_i |\psi_i(\vec{r})|^2$$

is given in terms of the one-electron wave functions $\psi_i(\vec{r})$, which depend nonlinearly on the effective one-electron potential $V(\vec{r})$. How this potential $V(\vec{r})$ also depends on the charge density ρ is also prescribed by density-functional theory, e.g., in the local-density approximation. The result is a nonlinear self-consistency problem for the charge density ρ or the potential V, which may be written in the form $\rho(\vec{r})=F_{\vec{r}}\{\rho\}$ or $V(\vec{r})=\tilde{F}_{\vec{r}}\{V\}$. Since other methods are not available, the solution must be found by iteration, e.g., $\rho_{N+1}(\vec{r})=F_{\vec{r}}\{\rho_N\}$.

Very often, however, this standard iteration diverges. During the iterations one obtains charge oscillations with increasing amplitude. Convergence can only be achieved if these oscillations are damped. In most applications one therefore applies a damping procedure by superimposing the input and output of the last iteration, i.e.,

$$\rho_{N+1}=\alpha F\{\rho_N\}+(1-\alpha)\rho_N \ .$$

By suitably choosing the parameter α, convergence is usually achieved. However, problems arise if the parameter α is chosen to be quite small in order to obtain convergence. Then the iteration process converges very slowly and many iterations are needed. For instance, in calculations for 3*d* impurities in noble metals,[2] typical α values are in the range 0.01—0.04; in extreme cases they can be even smaller. However, similar problems also arise in other situations. For instance, Koelling reports[3] that calculations for rare-earth metals, especially Ce, require $\alpha=0.05$—0.1. It is also known that calculations for ordered alloys require, in general, smaller mixing factors and more iterations than the calculations for the corresponding pure metals.

The aim of our paper is to discuss the origin and physical reason for these convergence problems and further, to find more efficient iteration procedures in cases where the simple mixing process $\rho_{N+1}=\alpha F\{\rho_N\}+(1-\alpha)\rho_N$ converges too slowly. Our paper essentially consists of two parts. In the first part, basically mathematical, we present a general discussion of the convergence of the standard iteration $\rho_{N+1}=F\{\rho_N\}$. Our method is based on a linearization of the self-consistency equations around the exact fixed-point solution. The matrix $f(\vec{r},\vec{r}')$, representing the functional derivative of $F_{\vec{r}}\{\rho\}$ with respect of $\rho(\vec{r}')$, is of central interest since its eigenvalues determine the convergence. An important restriction for the eigenvalues comes from the stability condition. In the second part we discuss improved iteration schemes. We first analyze the simple mixing procedure $\rho_{N+1}=\alpha F\{\rho_N\}+(1-\alpha)\rho_N$ and give some optimal choices for the mixing parameter α. In particular, we discuss the physical reason why the convergence of this method can be quite slow for certain systems. For such cases we propose a number of accelerated iteration schemes, which are all based on a more flexible use of mixing parameters. We illustrate these methods in calculations for 3*d* impurities in metals and show that they can be quite efficient.

Some of the material presented in this paper is in spirit similar to the work of Ferreira,[4] which came to our attention recently. However, our treatment is much more general. Furthermore, we should mention two more recent papers of Ho *et al.*[5] and Bendt and Zunger.[6] While our treatment is based on mixing parameters, these authors use techniques based on the Newton-Raphson method with considerable success.

II. LINEARIZATION OF THE SELF-CONSISTENCY EQUATION

In density-functional theory the charge density $\rho(\vec{r})$ can be expressed by the one-electron Green's function as a sum over all occupied states up to the Fermi energy:

$$\rho(\vec{r})=\frac{-2}{\pi}\int^{E_F} dE\ \mathrm{Im}G(\vec{r},\vec{r};E)=F_{\vec{r}}\{\rho\} \ . \qquad (1)$$

Since the Green's function is determined by the effective one-electron potential $V(\vec{r})$, which itself depends again on the density, we have a self-consistency condition $\rho=F\{\rho\}$. In order to study the convergence of the iteration process we linearize this equation around the exact fixed-point solution $\rho_*(\vec{r})$ for which $\rho_*=F\{\rho_*\}$. Using the Born approximation for the Green's function

$$G\cong G_*+G_*\,\delta V\,G_*,\quad \delta V=V-V_* \tag{2}$$

we obtain for the deviation $\delta\rho=\rho-\rho_*$

$$\delta\rho(\vec{r})=\int d\vec{r}\,'\chi(\vec{r},\vec{r}\,')\delta V(\vec{r})\,, \tag{3}$$

$$\chi(\vec{r},\vec{r}\,')=\frac{-2}{\pi}\int^{E_F} dE\,\mathrm{Im}[G_*(\vec{r},\vec{r}\,';E)G_*(\vec{r}\,',\vec{r};E)]\,. \tag{4}$$

$\chi(\vec{r},\vec{r}\,')$ is the susceptibility of independent electrons, being a real and symmetrical matrix. By linearization, δV is proportional to $\delta\rho$:

$$\delta V(\vec{r})=\int d\vec{r}\,'\,U(\vec{r},\vec{r}\,')\delta\rho(\vec{r}\,')\,, \tag{5}$$

$$U(\vec{r},\vec{r}\,')=\left.\frac{\delta V(\vec{r})}{\delta\rho(\vec{r}\,')}\right|_{\rho=\rho_*}=\left.\frac{\delta^2 W}{\delta\rho(\vec{r})\delta\rho(\vec{r}\,')}\right|_{\rho=\rho_*}$$
$$=\frac{1}{|\vec{r}-\vec{r}\,'|}+\left.\frac{d\mu_{\mathrm{xc}}(\rho(\vec{r}))}{d\rho}\right|_{\rho=\rho_*}. \tag{6}$$

Here W is the sum of the Hartree and exchange-correlation energies. The last equality holds in the local-density approximation, where μ_{xc} is the local exchange-correlation potential. Also, $U(\vec{r},\vec{r}\,')$ is real and symmetric. By combining (3) and (5), we obtain the linearized form of the self-consistency equation:

$$\delta\rho(\vec{r})=\int d\vec{r}\,'f(\vec{r},\vec{r}\,')\delta\rho(\vec{r}\,')\,,$$

with

$$f(\vec{r},\vec{r}\,')=\int d\vec{r}\,''\chi(\vec{r},\vec{r}\,'')U(\vec{r}\,'',\vec{r}\,')\,. \tag{7}$$

The kernel $f(\vec{r},\vec{r}\,')$ is just the functional derivative of $F_{\vec{r}}\{\rho\}$.

The standard iteration process $\rho_{N+1}=F\{\rho_N\}$ converges to the exact solution ρ_* if $\delta\rho_N\to 0$ for $N\to\infty$. By recursion we obtain for $\delta\rho_{N+1}$

$$\delta\rho_{N+1}=\underline{f}\delta\rho_N=\{\underline{f}\}^N\delta\rho_1=\sum_i\{\lambda_i\}^N|i_l\rangle\langle i_r|\,\delta\rho_1\,, \tag{8}$$

where we have used a spectral representation of $\underline{f}$ into its eigenvectors:

$$\underline{f}=\sum_i\lambda_i|i_l\rangle\langle i_r|\,,\quad\langle i_r|i_l\rangle=\delta_{ij}\,. \tag{9}$$

Since $\underline{f}$ is unsymmetric we must distinguish between the left and right eigenvectors $|i_r\rangle$ and $\langle i_l|$, which are mutually orthogonal. Later we will show that such a complete set of eigenvectors always exists and that the eigenvalues λ_i are real and smaller than $+1$ if the system is stable. Thus the standard iteration process converges if all eigenvalues λ_i are $|\lambda_i|<1$. Since for stability reasons $\lambda_i<+1$, we see that the iteration process diverges if $\lambda_i<-1$ or if $\lambda_i\to+1-0$, where the latter case corresponds to an instability.

Since the derivation above is based on linear response, the kernel $\underline{f}$ should be directly related to the static dielectric constant matrix $\underline{\epsilon}$ of the system. Indeed, it is easy to show that $\underline{\epsilon}$ is directly given by the transpose $\underline{f}^T$ of $\underline{f}$:

$$\underline{\epsilon}=\underline{1}-\underline{U}\,\underline{\chi}=\underline{1}-\underline{f}^T\,. \tag{10}$$

Redetermination of E_F. In the preceding discussion the Fermi energy E_F was considered as constant. This is justified for problems such as point defects, dislocations, surfaces, etc., where E_F is fixed by the bulk. However, if metal bulk properties are calculated, E_F must change in order to achieve neutrality. Then one has an additional term in Eqs. (3) and (7), i.e.,

$$\delta\rho_{N+1}(\vec{r})=\int d\vec{r}\,''d\vec{r}\,'\chi(\vec{r},\vec{r}\,'')U(\vec{r}\,'',\vec{r}\,')\delta\rho_N(\vec{r}\,')$$
$$+\rho(\vec{r},E_F)\delta E_F^{N+1}\,, \tag{11}$$

with

$$\rho(\vec{r},E_F)=\frac{-2}{\pi}\mathrm{Im}G_*(\vec{r},\vec{r};E_F)\,. \tag{12}$$

In each iteration E_F is determined anew by setting

$$\int_{V_c}d\vec{r}\,\delta\rho_{N+1}(\vec{r})=0=-\int_{V_c}d\vec{r}\,''\rho(\vec{r}\,'',E_F)U(\vec{r}\,'',\vec{r}\,')$$
$$\times\delta\rho_N(\vec{r}\,')+\rho(E_F)\delta E_F^{N+1}\,. \tag{13}$$

$\rho(E_F)$ is the density of states at the Fermi energy. For the susceptibility we have used the important sum rule

$$\rho(\vec{r}\,'',E_F)=-\int d\vec{r}\,\chi(\vec{r},\vec{r}\,'')\,, \tag{14}$$

which follows from (4) if we use the standard result $G^2=-\partial G/\partial E$. By inserting this result for δE_F^{N+1} into (11) we obtain again a recursion relation between $\delta\rho_{N+1}$ and $\delta\rho_N$ with the corresponding kernel given by

$$f(\vec{r},\vec{r}\,')=\int d\vec{r}\,''\chi(\vec{r},\vec{r}\,'')U(\vec{r}\,'',\vec{r}\,')$$
$$+\frac{\rho(\vec{r},E_F)}{\rho(E_F)}\int d\vec{r}\,''\rho(\vec{r}\,'',E_F)U(\vec{r}\,'',\vec{r}\,')\,. \tag{15}$$

The second term in (15) has a tendency to cancel the first since $\chi(\vec{r},\vec{r}\,'')$ is negative definite (as will be shown later), whereas the densities of states in the second term are positive. The cancellation is quite important and means that due to the readjustment of the Fermi energy during the iteration process, some possible strongly increasing oscillations of the total charge are prevented.

Equivalence of charge and potential iterations. Instead of considering the convergence of the charge, we may consider the convergence of the potential problem $V(\vec{r})=\tilde{F}_{\vec{r}}\{V\}$. From Eqs. (3) and (5) we obtain as a linearized equation

$$\delta V(\vec{r})=\int d\vec{r}\,' f^T(\vec{r},\vec{r}\,')\delta V(\vec{r}\,') ,$$

with (16)

$$\underline{f}^T=\underline{U}\,\underline{\chi}=\sum_i \lambda_i \,|\, i_r\rangle\langle i_l \,|\ .$$

The kernel $\underline{f}^T$ is the transpose of $\underline{f}$. In cases when E_F is redetermined during the iterations one must take the transpose of Eq. (15). In any case, $\underline{f}^T$ has the same eigenvalues λ_i as $\underline{f}$. Therefore the convergence of both the charge and the potential is the same, and it is sufficient to consider one of them. In the following we will therefore mostly consider the charge density. In practical applications, nevertheless, some slightly different convergence properties of the charge and potential might be observed. This could be due to nonlinearities at the beginning of the iteration process that are outside the frame of the present theory. Furthermore, a nonsymmetrical treatment of the potential and the charge, e.g., a muffin-tin approximation for the potential but not for the charge, might also lead to a somewhat different convergence.

Eigenvalues λ_i of the $\underline{f}$ matrix. During the iteration process the symmetry of the system is normally not changed, i.e., only those variations $\delta\rho(\vec{r})$ are allowed, which do not break the symmetry. Therefore only the submatrix $\underline{f}_\Gamma$ of $\underline{f}$ and its eigenvalues $\underline{\lambda}_i^\Gamma$ in the subspace Γ of full symmetry are needed. Thus for an ideal crystal where the eigenvectors can be classified by a Bloch vector $\vec{q}$, only charge variations with $\vec{q}=\vec{0}$ (point Γ) are considered. As a consequence, we expect the eigenvalues λ_i to form a discrete spectrum, even in an ideal crystal, since only the values at the Γ point are needed.

It is difficult to make predictions about the eigenvalues λ_i without specifying the system. However, a very general statement for λ_i follows from the stability of the system, as will be shown in the following.

We will restrict ourselves to situations where the Fermi energy is fixed by the bulk, so that the number of particles is not conserved. In this case we must consider the "grand-canonical" functional

$$E\{\rho\}=T_s\{\rho\}+W\{\rho\}-E_F\int d\vec{r}\rho(\vec{r}) , \tag{17}$$

where $T_s\{\rho\}$ is the kinetic energy of independent electrons and W the "potential" energy. ρ_* is determined by the vanishing of the first variation of $E\{\rho\}$. The second variation

$$\delta^2E=\tfrac{1}{2}\int d\vec{r}\,d\vec{r}\,'\,\delta\rho(\vec{r})[t_s(\vec{r},\vec{r}\,')+U(\vec{r},\vec{r}\,']\times\delta\rho(\vec{r}\,')>0 \tag{18}$$

is always positive if the system is stable or metastable, and vanishes for the exact solution $\delta\rho=0$. In Eq. (18) t_s is the second functional derivative of $T_s\{\rho\}$,

$$t_s(\vec{r},\vec{r}\,')=\left.\frac{\delta^2T_s}{\delta\rho(\vec{r})\delta\rho(\vec{r}\,')}\right|_{\rho=\rho_*}=t_s(\vec{r}\,',\vec{r}) , \tag{19}$$

whereas U is given by (6). The variation of δ^2E with respect to $\delta\rho$ gives the linearized self-consistency condition

$$\int t_s(\vec{r},\vec{r}\,')\delta\rho(\vec{r}\,')d\vec{r}\,'+\int d\vec{r}\,'\,U(\vec{r},\vec{r}\,')\delta\rho(\vec{r}\,')=0 . \tag{20}$$

By multiplication with $\underline{t}_s^{-1}$, this equation has the same form as Eq. (7), showing that $\underline{\chi}=-\underline{t}_s^{-1}$.

Now it is important that $t_s(\vec{r},\vec{r}\,')$ is positive definite, so that $\chi(\vec{r},\vec{r}\,')$ is negative definite. This follows from the positiveness of δ^2T_s, which can be seen by writing it in the Kohn-Sham form with the variations $\delta\psi_i$ of the wave functions

$$\delta^2T_s=\sum_i \tfrac{1}{2}\int d\vec{r}\,|\,\partial_{\vec{r}}\delta\psi_i(\vec{r})\,|^2>0 . \tag{21}$$

The connection with the eigenvalues λ_i introduced above is obtained as follows. Instead of $\delta\rho$ we use $\delta\tilde{\rho}=t_s^{1/2}\delta\rho$ as the new variable. Since t_s is positive definite, $t_s^{1/2}$ is well defined and positive definite as well. The energy variation δ^2E can then be written as

$$\delta^2E=\tfrac{1}{2}(\delta\tilde{\rho},(\underline{1}+\underline{t}_s^{-1/2}\underline{U}\,\underline{t}_s^{-1/2})\delta\tilde{\rho})>0 . \tag{22}$$

Thus the matrix $\underline{1}+\underline{t}_s^{-1/2}\underline{U}\,\underline{t}_s^{-1/2}$ is positive definite, real and symmetric; its eigenvalues μ_i are real and positive:

$$\underline{1}+\underline{t}_s^{-1/2}\underline{U}\,\underline{t}_s^{-1/2}=\sum_i \mu_i \,|\, i\rangle\langle i \,|\ , \quad \mu_i>0 . \tag{23}$$

By inserting this formula into (22), the energy change becomes a sum of the energies for the different "charge" modes $|\,i\rangle$:

$$\delta^2E=\sum_i \tfrac{1}{2}\mu_i \,|\,\langle i\,|\,\delta\tilde{\rho}\rangle\,|^2 . \tag{24}$$

Clearly, the case $\mu_i\to 0$ corresponds to an instability determined by the "soft" mode i. By multiplying Eq. (23) from the left with $\underline{t}_s^{-1/2}$ and from the right with $\underline{t}_s^{1/2}$, we obtain

$$\underline{1}+\underline{t}_s^{-1}\underline{U}=\underline{1}-\underline{f}=\sum_i \mu_i\underline{t}_s^{-1/2}\,|\,i\rangle\langle i\,|\,\underline{t}_s^{1/2}=\sum_i(1-\lambda_i)\,|\,i_l\rangle\langle i_r\,|\ . \tag{25}$$

Thus we see that the eigenvalues μ_i and λ_i are connected by $\mu_i=1-\lambda_i$ and that the left and right eigenvectors are given by $|\,i_l\rangle=\underline{t}_s^{-1/2}\,|\,i\rangle$ and $|\,i_r\rangle=\underline{t}_s^{1/2}\,|\,i\rangle$. We conclude that the eigenvalues $\mu_i=1-\lambda_i$ of the matrix $\underline{1}-\underline{f}$ and the dielectric constant matrix are real and positive. The limit $\mu_i\to 0+$ or $\lambda_i\to 1-0$ corresponds to an instability.

It is interesting to see that for the Hartree approximation, for which we neglect the exchange-correlation potential in (6), the $\underline{U}$ matrix is also positive. Then it follows from Eq. (23) that $\mu_i>1$ or $\lambda_i<0$. Thus the instabilities $\mu_i\to 0$ only occur due to exchange and correlation. On the other hand, in cases where these terms do not play a dominant role, we expect only the eigenvalues $\mu_i\gtrsim 1$ or $\lambda_i\lesssim 0$.

This discussion can easily be extended to the case of spin polarization where one must consider the densities $\rho_+(\vec{r})$ and $\rho_-(\vec{r})$ for both spin directions instead of the total density $\rho(\vec{r})$. The derivation is quite straightforward and analogous to the previous derivation. Especially from $\delta^2E>0$ the positiveness of all eigenvalues $\mu_i>0$ follows.

Two illustrative models. In the following we will dis-

cuss two simple models that illustrate the convergence problems of the self-consistency iterations. The two models eludicate two different reasons why the iteration process $\rho_{N+1}=F\{\rho_N\}$ can lead to convergence problems either due to large negative eigenvalues $\lambda_i \leq -1$ (or $\mu_i \geq 2$) as in the model for the 3*d* impurity or due to eigenvalues $\lambda_i \to 1-0$ ($\mu_i \to 0$), characterizing an instability as in the Stoner model.

3d impurity in jellium. In simple metals 3*d* impurities show a virtual bound state, i.e., a Lorentzian peak in the local density of states $n_{\rm loc}$ near the Fermi energy [Fig. 1(a)]. The position $E(n)$ of the resonance depends strongly on the number n of impurity d electrons, $E(n)=E_0+Un$, where U is the Coulomb integral. Thus increasing n shifts the peak above E_F and therefore depopulates it and vice versa. Thus n must satisfy the self-consistency condition

$$n=F(n)=2\int^{E_F} dE\, n_{\rm loc}(E-E_0-Un)\ , \tag{26}$$

which is schematically sketched in Figs. 1(b) and 1(c).

$F(n)$ is a monotonically decreasing function of n. $F(0)=10$ refers to a virtual bound state fully occupied by 10 *d* electrons; $F(\infty)=0$ means the peak is high above the Fermi energy and empty. The intersection of $F(n)$ with n determines the correct number n_* of impurity d electrons. In an iteration process one starts with a hypothesized number n_1, and calculates $n_2=F(n_1)$, etc. A graphical representation of this process is given in Figs. 1(b) and 1(c). Depending on the slope of $F(n)$ at n_* the iterations either converge as in Fig. 1(b) or diverge as in Fig. 1(c). This is in agreement with Eq. (8) since for a one-dimensional model there is only one eigenvalue, given by

$$\lambda=F'(n_*)=-2n_{\rm loc}(E_F-E_0-Un_*)U\ . \tag{27}$$

Divergence occurs for $F'(n_*)<-1$. From calculations for 3*d* impurities in noble metals, we can insert realistic numbers for U and $n_{\rm loc}(E_F)$ and obtain typically very large values for $F'(n_*)$ of the order of -50 to -100. Thus the process is strongly divergent, i.e., the charge oscillations induced by sweeping the virtual bound state back and fourth across the Fermi energy increase strongly in amplitude. Note that the charge oscillations would not occur if the Fermi energy could be readjusted during the iterations in order to achieve charge neutrality, as it is done in band-structure calculations for ideal crystals.

In the *Stoner model* of ferromagnetism the density of states for the spin-up and spin-down electrons are rigidly shifted with respect to each other by IM, where I is the exchange integral and M is the magnetization per atom [see Fig. 2(a)]. Thus a self-consistency condition for the moment M arises,

$$M=F(M)=\int^{E_F} dE[n(E+\tfrac{1}{2}IM)-n(E-\tfrac{1}{2}IM)]\ , \tag{28}$$

where $n(E)$ is the paramagnetic density of states. The function $F(M)$ increases monotonically from its value $F(0)=0$ to its maximal value $F(\infty)=5$ [Fig. 2(b)]. The intersection of $F(M)$ with the straight line M determines

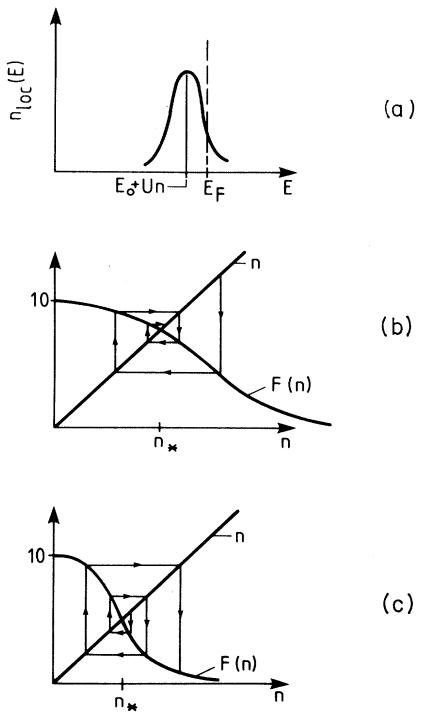

FIG. 1. (a) Local density of states of a 3*d* impurity in a simple metal (schematic). (b) Standard iteration process $n_{l+1}=F\{n_l\}$ converges: $|F'(n_*)|<1$. (c) Standard iteration process diverges: $|F'(n_*)|>1$.

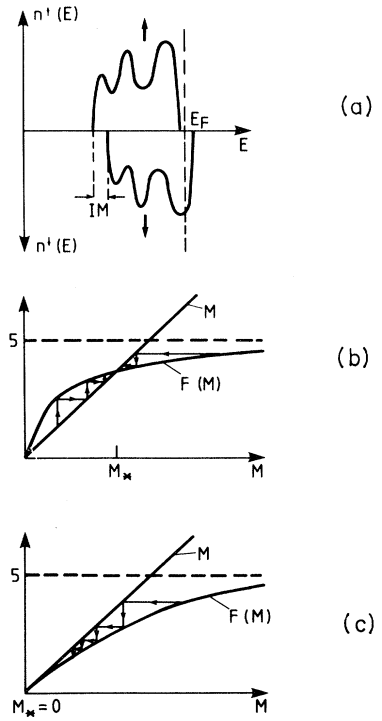

FIG. 2. (a) Schematic representation of the Stoner model. (b) Iteration process $M_{N+1}=F\{M_N\}$ converges, since $F'(M_*)<1$. (c) At the threshold the iteration process diverges, since $F'(M_*=0)=1$.

the correct value M_*. A sufficient condition for a nontrivial solution $M\neq 0$ is that the slope $F'(0)=n(E_F)I$ should be larger than 1, which is known as the Stoner criterion and which is assumed in Fig. 2(b). The iteration process $M_{N+1}=F(M_N)$ converges to the solution M_*, since $F'(M_*)<1$ and does not, in general, present a problem. However, near the threshold for the occurrence of a moment M_*, when $F'(0)=1$ as shown in Fig. 2(c), the convergence process is infinitely slow.

Both models are simple because only a single variable n or M must be determined self-consistently and because only a single eigenvalue [$F'(n_*)$ or $F'(M_*)$] determines the convergence. However, they realistically sketch the two physical situations for which convergence problems can occur: charge oscillations of localized d or f electrons with large densities of states and Coulomb integrals or instabilities, e.g., of magnetic origins. Of course, both complications can also occur simultaneously. This is illustrated in the following model for a magnetic impurity, where both the number of d electrons and the magnetization are to be determined:

$$\begin{aligned} n &= \int^{E_F} dE[\, n_{\rm loc}(E-E_0-Un+\tfrac{1}{2}IM) \\ &\qquad + n_{\rm loc}(E-E_0-Un-\tfrac{1}{2}IM]\,, \\ M &= \int^{E_F} dE[\, n_{\rm loc}(E-E_0-Un+\tfrac{1}{2}IM) \\ &\qquad - n_{\rm loc}(E-E_0-Un-\tfrac{1}{2}IM]\,, \end{aligned} \tag{29}$$

We will come back to this model in the next section.

III. THE SIMPLE MIXING PROCEDURE

Owing to the large charge oscillations that very often arise, the standard iteration process $\rho_{N+1}=F\{\rho_N\}$ is normally not used in realistic calculations. Instead, the dependable method that is used most often is a simple mixing procedure[7,8] where the input and output of the last iteration are superposed by a suitably chosen parameter α:

$$\rho_{N+1}(\vec{r})=\alpha F_{\vec{r}}\{\rho_N\}+(1-\alpha)\rho_N(\vec{r})\,. \tag{30}$$

It is readily seen that for each $\alpha\neq 0$ the correct solution ρ_* is obtained if the iteration process converges. While in principle $\alpha=\alpha(\vec{r})$ could be an arbitrary function of $\vec{r}$, in practice it is taken as a constant since no simple criterion specifying its $\vec{r}$ dependence is available. We will in this section analyze the convergence and the problems arising in the application of this method.

Setting $\rho_N=\rho_*+\delta\rho_N$ we obtain in analogy to the preceding section by linearization

$$\begin{aligned} \delta\rho_{N+1}(\vec{r}) &= \alpha\int d\vec{r}\,' f(\vec{r},\vec{r}\,')\delta\rho_N(\vec{r}\,')+(1-\alpha)\delta\rho_N(\vec{r}) \\ &= [1-\alpha(1-\underline{f})]^N\delta\rho_1 \\ &= \sum_i (1-\alpha\mu_i)^N\,|\,i_l\rangle\langle i_r\,|\,\delta\rho_1\,. \end{aligned} \tag{31}$$

For convergence all eigenvalues μ_i must satisfy

$$|\,1-\alpha\mu_i\,|<1\,. \tag{32}$$

This condition is illustrated in Fig. 3, where $1-\alpha\mu_i$ is plotted versus α. The resulting straight lines all fall between the limiting lines for the maximal and minimal eigenvalues $\mu_{\max}$ and $\mu_{\min}$. Since $\mu_i>0$ for stability reasons, all lines have a negative slope. One sees that the convergence is determined by the largest eigenvalue $\mu_{\max}$: For all α with $0<\alpha<2/\mu_{\max}$ the convergence is guaranteed. Note, however, that if $\mu_{\min}=0$ or if even $\mu_{\min}<0$, the process diverges. In order to obtain convergence in this case for the $\mu_{\min}$ component, a negative α value would be required, which, however, would destroy the convergence of the other eigenvectors with positive eigenvalues μ_i. Therefore unstable solutions of the Euler-Lagrange equation with $\delta^2E<0$ cannot be calculated by this method. An example for such a case is the Stoner model discussed in Sec. II. If the Stoner criterion $F'(0)>1$ is met, two degenerate and stable ferromagnetic solutions $\pm M_*$ and an unstable paramagnetic solution $M_*=0$ exist. From Fig. 2(a) one can convince oneself that the latter solution cannot be obtained by a mixing process with a positive α value.

Two choices for α are especially interesting: For $\alpha=1/\mu_{\max}$ the component of the eigenvector $|\,\mu_{\max}\rangle$ converges fastest, i.e., in the first step already if the linearization applies. However, the overall convergence is then determined by the small eigenvalues, since $1-\alpha\mu_{\min}$ is close to 1 and $(1-\alpha\mu_{\min})^N$ decreases most slowly with increasing N. An optimal compromise can be found by postulating that the components of the maximal and minimal eigenvalues should converge equally. The resulting $\alpha_{\rm opt}$ is slightly smaller than the convergence limit $2/\mu_{\max}$:

$$\begin{aligned} \alpha_{\rm opt} &= \frac{2}{\mu_{\max}+\mu_{\min}}\,, \\ R_{\rm opt} &= 1-\alpha_{\rm opt}\mu_{\min}\cong 1-2\frac{\mu_{\min}}{\mu_{\max}}\,. \end{aligned} \tag{33}$$

Both components then converge in powers of $R_{\rm opt}$. If large eigenvalues $\mu_{\max}$ or small eigenvalues $\mu_{\min}$ exist (examples given in Sec. II) the convergence is especially slow in particular if both conditions, $\mu_{\max}$ large and $\mu_{\min}$ small, occur simultaneously.

It is interesting to compare the convergence of the charge with the convergence of the total energy. By in-

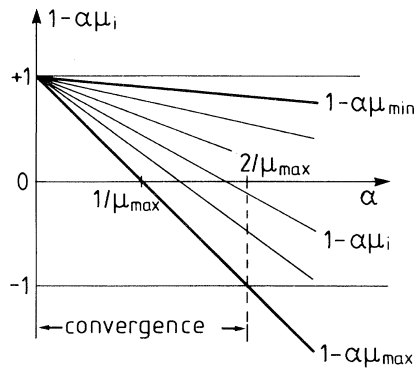

FIG. 3. Convergence of the simple mixing procedure $\rho_{N+1}=\alpha F(\rho_N)+(1-\alpha)\rho_N$ (see text).

serting Eq. (31) for $\delta\rho_{N+1}$ into Eq. (24) we obtain for $\delta^2 E_{N+1}$

$$\delta^2 E_{N+1}=\tfrac{1}{2}\sum_i \mu_i(1-\alpha\mu_i)^{2N}|\langle i_r|\delta\rho_1\rangle|^2 . \tag{34}$$

Thus the convergence of the energy proceeds in powers of $(1-\alpha\mu_i)^2$ instead of $1-\alpha\mu_i$ for the charge density. This means that the number of iterations necessary for the energy should be roughly a factor of 2 smaller than the number of iterations for the charge density. Note that the convergence of the energy can still be quite slow if $1-\alpha\mu_i$ is close to 1. This is contrary to the normal belief that the extremal properties of the total energy always ensure a fast convergence of the energy.

From the preceding discussion we must distinguish two different situations for which convergence problems can occur, i.e., $\mu_{\max}$ large or $\mu_{\min}$ small:

Large eigenvalues μ_{max}. Concluding from the model of the 3*d* impurity in Sec. II we expect large eigenvalues $\mu_{\max}$ in situations where we have large local densities of states at the Fermi energy and large Coulomb integrals and where, moreover, the Fermi energy is fixed by the host, for instance, *d* or *f* impurities, pairs of such impurities, similarly adatoms on surfaces, overlayers, etc. However, not only can the local impurity density of state determine the convergence, but the host density of states can also be of vital importance. We found such a situation to occur for *sp* impurities and the vacancy in Ni. In "single-site calculations"[9] where only the charge density and the potential at the impurity site are calculated self-consistently, the convergence was quite fast, as expected, since the local densities of states and the impurity Coulomb integrals are rather small for *sp* electrons. However, when in recent calculations[10] also charge perturbations at neighboring host sites were included, the convergence slowed down considerably and $\mu_{\max}$ values larger than 100 were found. Here the local density of states and the Coulomb integral at the neighboring host sites became decisive and determined the convergence. Therefore the coupling at more or less unperturbed host atoms can also cause problems if the host has a large density of states and a large Coulomb integral. Similar problems are also expected at surfaces when, e.g., the charge transfer between an adatom and the first host layer is included.

In an ideal crystal with one atom per unit cell the charge oscillations are, in general, suppressed due to the adjustment of the Fermi energy during the iteration process. However, problems can also arise if there are efficient intra-atomic charge-transfer processes leading to strong charge oscillations. For instance, Koelling[3] reports such problems for the band-structure calculations of Ce, where charge oscillations between the 4*f* and 5*d* shells occur that cannot be prevented by adjusting the Fermi energy, i.e., fixing the total number of electrons. Similar problems also occur for intermetallic compounds where the interatomic charge transfer plays a dominant role. In the following we present a simple model that illustrates these problems. We consider a two-component alloy with two atoms 1 and 2 per unit cell. Similar to the model for the 3*d* impurity we derive two coupled self-consistency conditions for the numbers N_1 and N_2 of electrons of both atoms:

$$\begin{aligned} N_1&=2\int^{E_F} dE\, n_1(E-E_{01}-U_{11}N_1-U_{12}N_2) ,\\ N_2&=2\int^{E_F} dE\, n_2(E-E_{02}-U_{22}N_2-U_{12}N_1) . \end{aligned} \tag{35}$$

Here U_{11} and U_{22} are the intra-atomic Coulomb integrals, $U_{12}=U_{21}$ is the interatomic Coulomb integral, whereas $n_1(E)$ and $n_2(E)$ are the local densities of states of both species. As in Sec. II we linearize these equations around the exact values N_1^* and N_2^*. From the condition of charge neutrality ($\delta N_1+\delta N_2=0$) the change δE_F of the Fermi energy can be evaluated. We obtain then one self-consistency condition for the charge-transfer process $\delta N_1=-\delta N_2$, the corresponding eigenvalue of which is given by

$$\mu=1-\lambda=1+\frac{2n_1(E_F)n_2(E_F)}{n_1(E_F)+n_2(E_F)}(U_{11}+U_{22}-2U_{12}) . \tag{36}$$

Two limiting cases are of special interest. For $n_2 \ll n_1$ and $U_{22}, U_{12} \ll U_{11}$ we obtain

$$\mu\cong 1+2n_2(E_F)U_{11} . \tag{37}$$

The E_F adjustment has the effect that μ is not given by $2n_1U_{11}$ but only by the smaller value $2n_2U_{11}$. However, if n_1 and n_2 as well as U_{11} and U_{22} are of equal magnitude, then this cancellation is not effective and μ is large. Of special interest is the case $n_1=n_2$ and $U_{11}=U_{22}$. This can be realized if one calculates a metal with a primitive unit cell using a band-structure program for a nonprimitive lattice, e.g., bcc Fe with a program for a CsCl structure with two atoms per unit cell. From Eq. (36) we obtain then $\mu=2n_1(E_F)U_{11}$, since U_{12} is normally smaller than U_{11}. Thus the E_F cancellation is not effective, and the same expression (27) as that for the 3*d* impurity is obtained. In a similar manner, these convergence problems for nonprimitive lattices have been noted in frozen-phonon calculations by Harmon and Ho[11] and are also discussed by Koelling.[3] The above-mentioned model can also be applied to the problem occurring for Ce if N_1 and N_2 are identified with the number of *f* and *d* electrons. The largest eigenvalue should then be given by (37), i.e., $\mu_{\max}\cong 2n_d(E_F)U_{ff}$.

Small eigenvalues μ_{min} correspond to a near instability of the system, which occurs at the onset or loss of new degrees of freedom. The most prominent instability is the threshold for a magnetic moment as illustrated by the Stoner model discussed in Sec. II. However, one can also think of other instabilities such as Jahn-Teller distortions, incommensurate charge- or spin-density waves, etc. One important feature of the magnetization problem (and presumably also of the other instabilities) is that near the threshold the charge density and the magnetization density decouple. This is essentially due to the fact that a small magnetic field cannot change the charge density if only linear effects are considered. Thus in first order the internal field created by the spontaneous magnetization does not couple to the charge density.

We will illustrate this point and its implications for the model of the magnetic impurity of Sec. II. Equation (29) gives two self-consistency conditions for the local charge n and the local moment M of the impurity. By expanding around the exact solutions n_*, M_* we obtain the linear equations

$$\begin{bmatrix} \delta n \\ \delta M \end{bmatrix}_{N+1} = \underline{f} \begin{bmatrix} \delta n \\ \delta M \end{bmatrix}_N , \tag{38}$$

with

$$\underline{f} = \begin{bmatrix} -(n^\uparrow + n^\downarrow)U & \frac{1}{2}(n^\uparrow - n^\downarrow)I \\ -(n^\uparrow - n^\downarrow)U & \frac{1}{2}(n^\uparrow + n^\downarrow)I \end{bmatrix} ,$$

where $n^\uparrow$ and $n^\downarrow$ refer to the local density of states at E_F for both spin directions. Near the threshold for the occurrence of a local moment one has $|n^\uparrow - n^\downarrow| \ll n^\uparrow + n^\downarrow$ so that the two eigenvalues $\lambda_{1,2}$ that determine the convergence are given by

$$\begin{aligned} \lambda_1 &\cong -(n^\uparrow_{\rm loc} + n^\downarrow_{\rm loc})U , \\ \lambda_2 &\cong +(n^\uparrow_{\rm loc} + n^\downarrow_{\rm loc})I/2 . \end{aligned} \tag{39}$$

In this limit the two eigenvalues coincide with the diagonal elements of $\underline{f}$, showing that the coupling between δn and δM is not important. Moreover, the highest eigenvalue λ_1 is to first order in M_* independent of the fixed-point magnetization and equal to the paramagnetic eigenvalue at the threshold $M_* = 0$. Thus the convergence of the charge density is decoupled from the convergence of the magnetization near the threshold. Since near the threshold $\lambda_2 \approx n_{\rm loc}(E_F - Un_*)I$ approaches 1, only the convergence of the magnetization is slowed down, while the convergence of the charge density is unaffected and essentially equal to the convergence behavior in a paramagnetic calculation.

IV. SOME ACCELERATED ITERATION SCHEMES

Owing to the problems that arise when the simple mixing scheme is used in certain physical situations it is of importance to find improved iteration schemes that are at least partially free of these limitations. Some promising schemes will be discussed in the following. Most of these are based on a more flexible use of mixing parameters than in the simple mixing procedure. At the end of this section these schemes will be applied in realistic calculations for $3d$ impurities in Cu.

A. Extrapolation by geometrical series

After many iterations in the simple mixing procedure [Eq. (31)], only the slowest converging eigenvector remains, i.e., the eigenvector for which $1-\alpha\mu_i$ is closest to 1 (usually $\mu_{\rm min}$; see Fig. 3). Therefore one has for large N a scalar relationship between $\delta\rho_{N+1}(\vec{r})$ and $\delta\rho_N(\vec{r})$, i.e.,

$$\delta\rho_{N+1}(\vec{r}) \cong \beta\delta\rho_N(\vec{r}) \cong \beta^2\delta\rho_{N-1}(\vec{r}) ,$$

with

$$\beta = 1 - \alpha\mu_{\rm min} . \tag{40}$$

By setting $\delta\rho_{N+1}(\vec{r}) = \rho_{N+1}(\vec{r}) - \rho_*(\vec{r})$ and by eliminating β from the above equations, the limiting value $\rho_*(\vec{r})$ can be estimated from successive iterations:

$$\rho_*(\vec{r}) \cong \frac{\rho_{N+1}\rho_{N-1} - (\rho_N)^2}{\rho_{N+1} - 2\rho_N + \rho_{N-1}} . \tag{41}$$

For self-consistency problems with a single variable this formula is identical with Aitken's δ^2 process.[7,8] One can also show that it can be considered as an extrapolation by a geometrical series starting from the iteration ρ_N. By introducing the deviation $\Delta\rho_{N+l} = \rho_{N+l} - \rho_N$ from ρ_N as the new variable, one obtains the recursion formula

$$\begin{aligned} \Delta\rho_{N+l} &= \beta\Delta\rho_{N+l-1} + \Delta\rho_{N+1} \\ &= \frac{1-\beta^l}{1-\beta}\Delta\rho_{N+1}, \quad l \geq 1 \end{aligned} \tag{42}$$

or, for $l \to \infty$,

$$\rho_*(\vec{r}) = \rho_N(\vec{r}) + \frac{1}{1-\beta}[\rho_{N+1}(\vec{r}) - \rho_N(\vec{r})] . \tag{43}$$

The factor β can be determined from the last three iterations, yielding

$$\beta = \frac{\rho_{N+1}(\vec{r}) - \rho_N(\vec{r})}{\rho_N(\vec{r}) - \rho_{N-1}(\vec{r})} . \tag{44}$$

By introducing β into (43) we obtain the same result as above. In the asymptotic region, β should be independent of $\vec{r}$. In practice, there will be a slight $\vec{r}$ dependence. Moreover, β is the ratio of two small quantities. For both reasons it may be of advantage to use Eq. (43) instead of (41) and take an average β by integrating out the $\vec{r}$ dependence.

B. The method of Anderson

Linear combinations of the inputs ρ_N, ρ_{N-1} and the outputs $F\{\rho_N\}, F\{\rho_{N-1}\}$ of two successive iterations are formed in order to determine an optimized input $\tilde{\rho}_N$ and output $\tilde{F}_N$:

$$\begin{aligned} \tilde{\rho}_N &= \alpha_N\rho_N + (1-\alpha_N)\rho_{N-1} , \\ \tilde{F}_N &= \alpha_N F\{\rho_N\} + (1-\alpha_N)F\{\rho_{N-1}\} . \end{aligned} \tag{45}$$

Ideally, α_N should be determined such that $\tilde{F}_N = \tilde{\rho}_N$. However, this cannot be realized by a simple parameter α_N since $\tilde{\rho}_N(\vec{r})$ and $\tilde{F}_N(\vec{r})$ are functions of $\vec{r}$. Instead in each iteration α_N is determined so that the least-squares deviation of $\tilde{\rho}_N$ and $\tilde{F}_N$,

$$\int d\vec{r}\,[\tilde{F}_N(\vec{r}) - \tilde{\rho}_N(\vec{r})]\,|^2 \equiv (\tilde{F}_N - \tilde{\rho}_N, \tilde{F}_N - \tilde{\rho}_N) , \tag{46}$$

is minimized, yielding an optimal mixing parameter α_N in each iteration:

$$\alpha_N = -\frac{(r_{N-1}, r_N - r_{N-1})}{(r_N - r_{N-1}, r_N - r_{N-1})} ,$$

with

$$r_N = F_N - \rho_N . \tag{47}$$

One can also modify the least-squares condition by introducing a suitable weighting factor $W(\vec{r})$ in the integral (46) corresponding to a different metric for the scalar product.

As discussed by Anderson,[12] it is often necessary to introduce an additional mixing factor α' to construct the input ρ_{N+1} of the next iterations:

$$\rho_{N+1}=\alpha'\tilde{F}_N+(1-\alpha')\tilde{\rho}_N \ . \tag{48}$$

Setting $\alpha'=1$ can cause convergence problems. The method has also been generalized[12] to include the information of more than two iterations.

C. Iteration cycles

Whereas in the simple mixing scheme the factor α is kept constant during all iterations, in the method of Anderson α_N is redetermined in each iteration. An alternative to these extremes is iteration cycles with different periodically repeated mixing factors. The simplest case are cycles with two mixing factors α and β:

$$\begin{aligned}\rho_{2N+1}&=\alpha F\{\rho_{2N}\}+(1-\alpha)\rho_{2N} \ ,\\ \rho_{2N+2}&=\beta F\{\rho_{2N+1}\}+(1-\beta)\rho_{2N+1} \ .\end{aligned} \tag{49}$$

By linearization, we obtain for two subsequent cycles

$$\delta\rho_{2N+2}=\sum_i (1-\beta\mu_i)(1-\alpha\mu_i)\,|\,i_l\rangle\langle i_r\,|\,\delta\rho_{2N} \ . \tag{50}$$

An optimization of these mixing factors seems to require a detailed knowledge of the spectrum of eigenvalues μ_i. If only two eigenvalues μ_1 and μ_2 exist, the choice $\alpha=1/\mu_1$ and $\beta=1/\mu_2$ guarantees a convergence after one cycle. If only the highest and lowest eigenvalues of the spectrum are known, the Tschebyscheff acceleration method[7] represents an elegant and optimized solution. If the spectrum consists of one dominating, very large eigenvalue $\mu_{\max}$ and many other smaller eigenvalues, as it is the case, e.g., for $3d$ impurities in metals, the component of the largest eigenvector $|\mu_{\max}\rangle$ converges very fast if α is choosen as $\alpha\cong 1/\mu_{\max}$. For the second iteration the mixing factor β can therefore be much larger than α. For instance, if α is exactly equal to $1/\mu_{\max}$, convergence is achieved for all $\beta<2/\mu_{\max}^{(2)}$, where $\mu_{\max}^{(2)}\ll\mu_{\max}$ is the second highest eigenvalue. The method requires a rather accurate knowledge of $\mu_{\max}$ since for a fast convergence $|(1-\alpha\mu_{\max})(1-\beta\mu_{\max})|\ll 1$ must be satisfied.

D. Problems connected with spin polarization

As discussed in Sec. III special problems arise in the case of spin polarization if the system is near the threshold for the occurrence of a magnetic moment. Then the minimal eigenvalue $\mu_{\min}$ approaches zero, which slows down the convergence. In this case one can take advantage of the fact that near the threshold the magnetization density and the charge density decouple, which means that only the convergence of the magnetization is slowed down. To a large extent this problem can be overcome by introducing two different mixing factors α_ρ and α_m for the charge ρ and the magnetization m:

$$\begin{aligned}\rho_{N+1}(\vec{r})&=\alpha_\rho F^{(\rho)}\{\rho_N,m_N\}+(1-\alpha_\rho)\rho_N(\vec{r}) \ ,\\ m_{N+1}(\vec{r})&=\alpha_m F^{(\rho)}\{\rho_N,m_N\}+(1-\alpha_m)m_N(\vec{r}) \ .\end{aligned} \tag{51}$$

Since charge and magnetization are decoupled for $\mu_{\min}\to 0$, the final convergence proceeds in powers of $1-\alpha_m\mu_{\min}$ instead of $1-\alpha_\rho\mu_{\min}$ if only one mixing factor α_ρ is used. Therefore an improved convergence is obtained if α_m is chosen as $\alpha_m\gg\alpha_\rho$, which is possible since the maximal eigenvalue for the magnetization problem is, according to our experience, much smaller than that for the charge problem (i.e., $\mu_{\max}$).

E. Increasing the exchange-correlation potential

The following procedure, suggested by Harris,[13] tries to reduce the largest eigenvalue $\mu_{\max}$. The idea is to split the one-electron potential $V(\vec{r})$ into the Coulomb part V_C and the exchange-correlation part $V_{\rm xc}$ and to mix both during the iterations with different factors α_C and $\alpha_{\rm xc}$:

$$\begin{aligned}V_{N+1}^{C}&=\alpha_C F_C\{V_N\}+(1-\alpha_C)V_N^C \ ,\\ V_{N+1}^{\rm xc}&=\alpha_{\rm xc}F_{\rm xc}\{V_N\}+(1-\alpha_{\rm xc})V_N^{\rm xc} \ ,\end{aligned} \tag{52}$$

with $V=V^C+V^{\rm xc}$. Here F_C and $F_{\rm xc}$ are the output Coulomb and exchange-correlation potentials of the Nth iteration. Since the exchange-correlation potential $V_{\rm xc}$ is negative, thus opposite in sign to the electron-electron interaction contained in V_C, the choice $\alpha_{\rm xc}>\alpha_C$ should accelerate the convergence. For instance, for the models discussed in Sec. II the Coulomb integral $U=U_C+U_{\rm xc}$ would effectively by replaced

$$U_{\rm eff}=U_C+\frac{\alpha_{\rm xc}}{\alpha_C}U_{\rm xc}<U \ ,$$

so that effectively the largest eigenvalues $\mu_{\max}$ and consequently the violent charge oscillations during the iterations could be diminished. Since we are dealing with localized electrons, the optimal ratio $\alpha_{\rm xc}/\alpha_C$ should be more or less an atomic property so that different choices for different atoms could be of advantage.

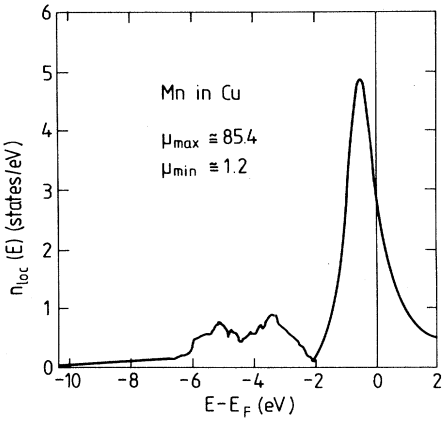

FIG. 4. Local density of states for a nonmagnetic Mn impurity in Cu.

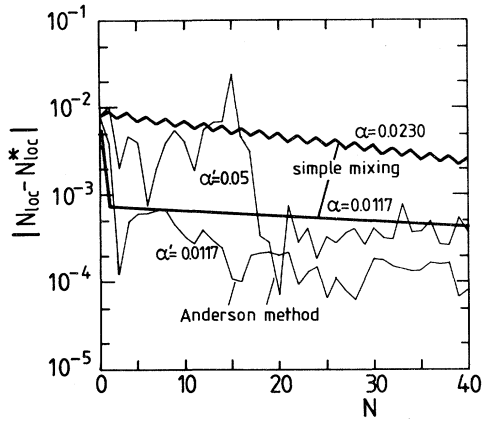

FIG. 5. Convergence of the deviation $|N_{\rm loc}-N^*_{\rm loc}|$ of the local impurity charge from the exact value versus the number of iterations N. Thick lines, simple mixing procedure; thin lines, Anderson's method. A judiciously chosen starting potential with $|N_{\rm loc}-N^*_{\rm loc}| \cong 10^{-2}$ at the beginning has been chosen.

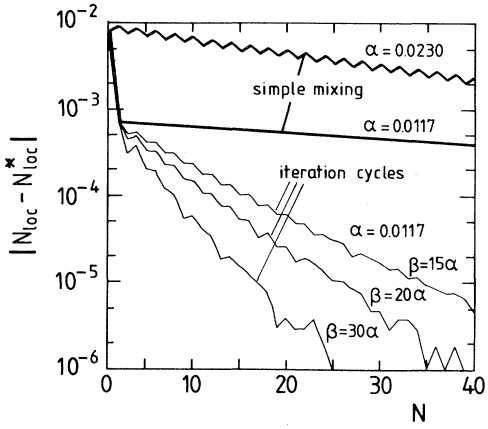

FIG. 7. Convergence of the impurity charge vs the number N of iterations. Thick lines, simple mixing procedure (same as Fig. 5); thin lines, iteration cycles. The judiciously chosen starting potential of Fig. 5 has been chosen.

F. Test calculations for 3*d* impurities in Cu

We have tested some of the previous iteration schemes for calculations of 3*d* impurities in Cu. In these calculations we apply density-functional theory in the local-density approximation of Hedin and Lundqvist[14] or von Barth and Hedin[15] for the spin-polarized case. We assume a muffin-tin approximation for the effective one-electron potentials. Perturbed potentials at the impurity site and at the neighboring host sites are allowed and calculated self-consistently. The calculations are based on the Korringa-Kohn-Rostoker (KKR) Green's-function method, which is able to take all band-structure effects of the host into account. For details, we refer to Refs. 10 and 16.

As an example, Fig. 4 shows the local density of states for a Mn impurity in Cu (fully converged solution) in the nonmagnetic spin-restricted calculation. A strong virtual bound state at the Fermi energy and considerable intensity within the range of the Cu *d* band between -2 and -6 eV are found, resulting from the hybridization of the impurity *d* electrons with the *d* electrons of the Cu neighbors. From the large density of states at E_F and the large Coulomb integral of the 3*d* electrons, we expect a very large maximal eigenvalue $\mu_{\rm max}$, which we have estimated as follows. Starting from a fairly well-converged solution, we apply the simple mixing scheme and increase the mixing parameter α until the solution diverges. Since all other eigenvalues are considerably smaller than $\mu_{\rm max}$ (see below), for $\alpha \gtrsim 2/\mu_{\rm max}$ only the component of $|\mu_{\rm max}\rangle$ diverges $\sim(1-\alpha\mu_{\rm max})^N$. In this way $\mu_{\rm max}$ can be determined quite accurately as $\mu_{\rm max}=85.4$. From the final convergence the lowest eigenvector can be estimated as $\mu_{\rm min}\cong 1.2$.

The convergence of the simple mixing procedure is illustrated in Figs. 5 and 6, which show on a semilogarithmic scale the deviation $|N_{\rm loc}-N^*_{\rm loc}|$ versus the iteration number N. $N_{\rm loc}$ refers to the local number of electrons in the Mn cell, and $N^*_{\rm loc}$ is the fully converged value. Two special choices for α have been chosen: $\alpha=1/\mu_{\rm max}=0.0117$ and $\alpha_{\rm opt}=2/(\mu_{\rm max}+\mu_{\rm min})=0.0230$. In Fig. 5 we have taken a judiciously chosen impurity potential from a fairly converged solution as a starting point

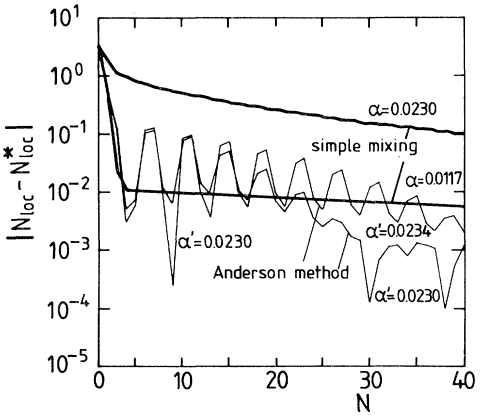

FIG. 6. Same as Fig. 5 but with poorly chosen starting potential ($|N_{\rm loc}-N^*_{\rm loc}| \approx 3$ at the beginning).

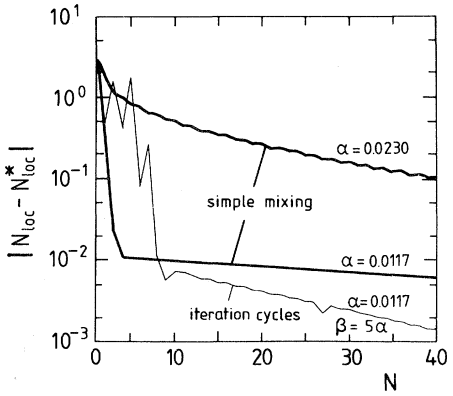

FIG. 8. Same as Fig. 7, but with poorly chosen starting potential of Fig. 6.

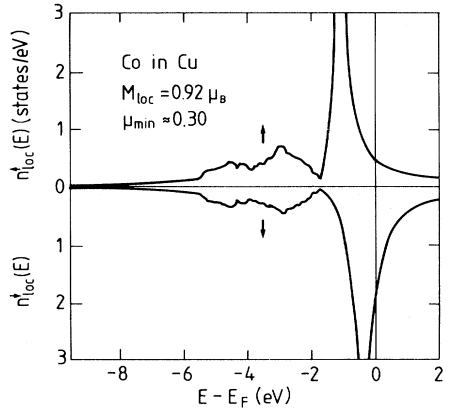

FIG. 9. Local density of states for both spin directions of a Co impurity in Cu.

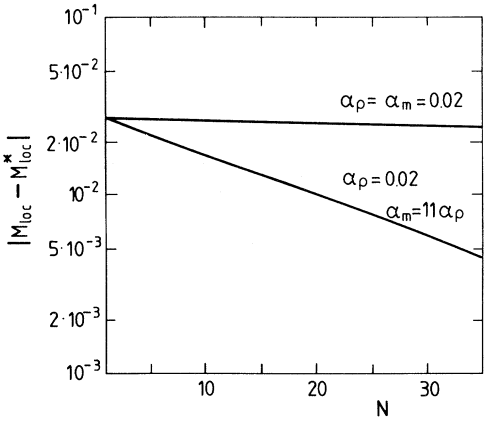

FIG. 10. Acceleration of the convergence of the local Co moment by using different mixing parameters α_ρ and α_m for the charge and magnetization.

so that $|N_{loc}-N^*_{loc}|\cong 10^{-2}$ at the beginning. In contrast, in Fig. 6 a poorly chosen impurity potential with $|N_{loc}-N^*_{loc}|\cong 3$ has been chosen as a starting potential. In both cases $\alpha=1/\mu_{max}\cong 0.0117$ leads to a very fast initial convergence followed by a rather slow improvement later. This shows the dominant behavior of the largest eigenvector μ_{max}, which converges after a few iterations and dramatically improves the local charge. Compared to this the subsequent slow improvements due to the convergence of all other eigenvectors are rather small. Nevertheless, they are important in order to obtain a well-converged solution. For the larger α value $\alpha=\alpha_{opt}\cong 0.0230$ the convergence is more steady and slow since now all components converge about equally slow. Nevertheless, the final convergence is faster for this α value since the slope of the curve is about a factor of 2 larger. However, it takes more than 100 iterations before this ultimately faster method becomes worthwhile. A simple improvement would be to take initially $\alpha=1/\mu_{max}$ and then increase α to $\alpha_{opt}\approx 2/\mu_{max}$. For both α values the curves are rather straight after 10—20 iterations, so that the final result can be extrapolated reasonably well by a geometrical series.

Included in Figs. 5 and 6 are also iterations based on the Anderson scheme (thin lines). The values for α' refer to the additional mixing parameter α' of Eq. (48). In all our applications of this method the convergence is quite erratic. It can improve dramatically within a few iterations and can just as well get worse again afterwards. In general, it seems to be difficult to optimize or to smooth the result obtained with this method. Nevertheless, it works and in most cases we studied, the overall convergence was faster than that of the simple mixing scheme.

Figures 7 and 8 show test calculations using iteration cycles again for two initial conditions $|N_{loc}-N^*_{loc}|\cong 10^{-2}$ (Fig. 7) and $|N_{loc}-N^*_{loc}|\cong 3$ (Fig. 8). For comparison, we have also included the results of the simple mixing scheme for $\alpha=1/\mu_{max}$ and $\alpha=2/(\mu_{max}+\mu_{min})$ (thick lines, same curves as in Figs. 5 and 6). We have taken two elementary iterations per cycle, one with $\alpha=1/\mu_{max}=0.0117$ and the second with a considerably larger β value. It is seen that the convergence is very fast, becoming faster with larger β. From the fact that even the cycles with $\beta=30\alpha$ converge, one can conclude that the second highest eigenvalue $\mu^{(2)}_{max}$ is smaller than $\mu_{max}/15$. While this method shows a very fast convergence, it has the drawback that one needs an accurate value of μ_{max} to start converging iteration cycles.

Finally, we want to discuss spin-polarized calculations for $3d$ impurities in Cu. Figure 9 shows the local density of states for both spin directions of a Co impurity in Cu (Ref. 10) for which the calculations give a local moment of $0.92\mu_B$ and correspondingly a spin-split virtual bound state. The minimum eigenvalue is estimated as $\mu_{min}\cong 0.30$, i.e., Co is close to the threshold corresponding to $\mu_{min}=0$. Figure 10 illustrates the acceleration of the convergence of the local moment $(M_{loc}-M^*_{loc})$ if different mixing factors α_ρ and α_m are used. Whereas for $\alpha_\rho=\alpha_m=0.02$ the convergence of the magnetization is quite slow, this is considerably improved if $\alpha_m\gg\alpha_\rho$ is chosen.

V. CONCLUSIONS

We have given a rigorous analysis of the convergence of self-consistency iterations in electronic structure calculations that is based on a linearization of the self-consistency equations around the exact solution. The convergence is critically determined by the eigenvalues μ_i of the dielectric constant matrix $\underline{\epsilon}$, which are positive for stable or metastable systems. In particular, we have studied the usual mixing procedure $\rho_{N+1}=\alpha F\{\rho_N\}+(1-\alpha)\rho_N$ and have shown that this procedure converges, provided $\alpha<2/\mu_{max}$. However, the convergence can be quite slow if either very large eigenvalues μ_{max} or/and very small eigenvalues μ_{min} exist.

Large eigenvalues μ_{max} can occur for systems with strongly localized d or f electrons and are due to large densities of states at the Fermi energy and large Coulomb integrals. These systems are characterized by violent charge oscillations during the iteration process. A simple example is the model of the $3d$ impurity in Sec. II. However, as explained in Sec. III similar problems can also

occur in ordered alloys, where one may have charge-transfer oscillations, or even in elemental metals like Ce, where the charge can fluctuate between the f and d shell.[3]

In contrast, small eigenvalues $\mu_{\min} \to 0+$ are connected with instabilities of the system and always occur near the threshold for the occurrence of a local moment. The simplest example is the Stoner model of ferromagnets as discussed in Sec. II.

We have also proposed some improved iteration schemes for cases where the simple mixing procedure converges too slowly. These schemes allow more flexible use of mixing parameters than the simple mixing procedure, e.g., a different mixing parameter in each iteration as in the Anderson method, different mixing parameters during iteration cycles, or two different mixing parameters, for instance, one for the charge and one for the magnetization. Some of these methods have been tested in realistic calculations for $3d$ impurities in Cu and can lead to considerable savings of computer time. Compared to recent techniques[5,6] based on the Newton-Raphson method, they are easier to implement in existing computing routines.

ACKNOWLEDGMENTS

We would like to acknowledge helpful discussions with A. R. Williams and R. Podloucky during the early stages of this work.

[1]P. C. Hohenberg and W. Kohn, Phys. Rev. 136, B864 (1964); W. Kohn and L. J. Sham, *ibid.* 140, A1133 (1965).
[2]R. Podloucky, R. Zeller, and P. H. Dederichs, Phys. Rev. B 22, 5777 (1980).
[3]D. D. Koelling, Rep. Prog. Phys. 44, 155 (1981).
[4]L. G. Ferreira, J. Comp. Phys. 36, 198 (1980).
[5]K. M. Ho, J. Ihm, and J. D. Joannopoulos, Phys. Rev. B 25, 4260 (1982).
[6]P. Bendt and A. Zunger, Phys. Rev. B 26, 3114 (1982).
[7]G. I. Marchuk, *Methods of Numerical Mathematics* (Springer, New York, 1975), Chap. 3.
[8]E. Isaacson and H. B. Keller, *Analysis of Numerical Methods* (Wiley, New York, 1972), Chap. 3.
[9]R. Zeller, *Physics of Transition Metals, 1980,* edited by P. Rhodes (Institute of Physics, London, 1980), p. 265
[10]P. J. Braspenning, R. Zeller, A. Lodder, and P. H. Dederichs, Phys. Rev. B (in press).
[11]B. N. Harmon and K. M. Ho, in *Superconductivity of d- and f-Band Metals,* edited by H. Suchland and M. B. Maple (Academic, New York, 1979), p. 173.
[12]D. G. Anderson, J. Assoc. Comput. Mach. 12, 547 (1964).
[13]J. Harris (private communication).
[14]L. Hedin and B. I. Lundqvist, J. Phys. C 4, 2064 (1971).
[15]U. von Barth and L. Hedin, J. Phys. C 5, 1629 (1972).
[16]R. Zeller and P. J. Braspenning, Solid State Commun. 42, 701 (1982).